

Study of toponium production including the effects of Higgs-boson exchange

J. Feigenbaum*

Physics Department, Case Western Reserve University, Cleveland, Ohio 44106

(Received 20 August 1990)

The production rates for toponium in e^+e^- collisions are calculated for a top-quark mass in the range of 100–200 GeV including the effects of standard-model Higgs-boson exchange. The effects due to this exchange fall off rapidly with the Higgs-boson mass, but lead to changes comparable to those due to uncertainties in Λ for a light Higgs boson.

I. INTRODUCTION

It has long been hoped that the study of toponium would allow the measurement of the QCD parameter Λ , which would, in turn, refine our knowledge of the interquark potential.¹ These hopes were, in part, based on the expectation that the top quark is lighter than the W so that there would be a large number (≈ 20) of narrow S -wave states.

Recent results, however, have established a lower bound on the top-quark mass $m_t \geq 89$ GeV.² The currently favored range seems to be $m_t = 140 \pm 40 \pm 20$ GeV.³

These results imply that expectations for top-quark spectroscopy must be revised. Most importantly, the width of the top quark increases rapidly due to decays into real W 's. Thus, the distance between successive toponium states is typically smaller than the width of the states, so all but the first one or two bound states overlap and become indistinguishable.^{4,5}

Also, interactions other than QCD become important. The Higgs-boson exchange rapidly becomes an important correction to QCD since it increases with m_t .^{6,7} Previous studies have included the Higgs-boson exchange in their analysis of quarkonia, but these were generally concerned with ultraheavy quarks with masses on the order of 1 TeV which might be members of fourth or higher generations.^{8,9} Thus, their results have little immediate application to toponium if m_t is in the presently accepted range.

This report describes the results of calculations of

both the cross section and energy eigenvalues of toponium states using an interquark potential involving only one-gluon exchange¹⁰ as well as the Wisconsin¹¹ and Richardson¹² potentials. (For a discussion of these potentials see Refs. 13 and 14.) We confine ourselves mainly to the case $m_t = 140$ GeV. The effects of the Higgs-boson exchange are included for different values of the Higgs-boson mass m_H . The results of shifts in either Λ or m_H on the graphs of the cross section are compared. The calculations of energy eigenvalues from the potential models are used as a check on the production plots.

II. CROSS-SECTION CALCULATIONS

The ratio of $\sigma_{t\bar{t}}$ to $\sigma_{\mu\bar{\mu}}$, $R_{t\bar{t}}$, has been calculated by Fadin and Khoze:¹⁰

$$R_{t\bar{t}} = \frac{9}{2} \frac{4\pi}{m_t^2} \left(Q_t^2 + \frac{v_t^2}{\kappa(1 - M_W^2/4m_t^2)^2} \right) \frac{1 + \frac{3}{4}\beta}{[1 - \mathcal{P}(4m_t^2)]^2} \times \int_0^1 dx \operatorname{Im} G_{E - m_t x^{1/\beta} + i\Gamma_t}(0, 0), \quad (1)$$

where

$$\begin{aligned} \beta &= (4\alpha/\pi) \left[\ln \left(\frac{2m_t}{m_e} \right) - \frac{1}{2} \right], \\ v_t &= 1 - \frac{8}{3} \sin^2 \theta_W, \\ \kappa &= (16 \sin^2 \theta_W \cos^2 \theta_W)^2, \end{aligned} \quad (2)$$

$Q_t = \frac{2}{3}$, and $\mathcal{P}(4m_t^2) \approx 0.07$. The imaginary part of the Green's function is¹⁰

$$\operatorname{Im} G_{E+i\Gamma_t}(0, 0) = \frac{m_t^2}{4\pi} \left(\frac{k_+}{m_t} + \frac{2\bar{k}_1}{m_t} \arctan \frac{k_+}{k_-} + \sum_{n=1}^{\infty} \frac{2\bar{k}_1}{m_t^2 n^4} \frac{\Gamma_t \bar{k}_1 n + k_+ (n^2 \sqrt{E^2 + \Gamma_t^2} + \bar{k}_1^2/m_t)}{(E + \bar{k}_1^2/m_t n^2)^2 + \Gamma_t^2} \right), \quad (3)$$

with $\bar{k}_1 = \frac{2}{3}\alpha_s m_t$,

$$k_{\pm} = \left(\frac{m_t}{2} (\sqrt{E^2 + \Gamma_t^2} \pm E) \right)^{1/2},$$

and $E = \sqrt{s} - 2m_t$. The width of the top quark for decay into W bosons¹⁵ is

$$\Gamma_t \equiv \frac{G_F m_t^3}{8\pi\sqrt{2}} \left(\frac{2P_W}{m_t} \right) \left[\left(1 - \frac{m_b^2}{m_t^2} \right)^2 + \left(\frac{m_b^2 M_W^2 - 2M_W^4}{m_t^4} \right) + \left(\frac{M_W}{m_t} \right)^2 \right], \quad (4)$$

where

$$P_W = \frac{[m_t^2 - (M_W + m_b)^2]^{1/2} [m_t^2 - (M_W - m_b)^2]^{1/2}}{2m_t}.$$

The first term in Eq. (3) corresponds to the Born approximation (modified by finite-width effects); the second term is a loop contribution, while the third term is a sum over S -wave bound states which have a width of $2\Gamma_t$. The inclusion of this last term allows one to study resonance effects and was neglected in the calculation of Sher and Silverman.⁶

The above expressions were derived on the basis of one-gluon exchange with fixed α_s . We can take into account the effects of running α_s by replacing α_s by

$$\alpha_s(E) = 4\pi \{7.67 \ln[m_t(E^2 + \Gamma_t^2)^{1/2}/\Lambda^2]\}^{-1} \quad (5)$$

in the above expressions.¹⁰

In order to use other potentials, an effective α_s can be determined and substituted back into Eq. (3). For example, to include the effects of the Higgs-boson exchange, the effective α_s is obtained by adding a second term,

$$\Delta\alpha_s(E) = \frac{3}{4} \frac{m_t^2 \sqrt{2} G_F}{4\pi} \frac{m_t(E^2 + \Gamma_t^2)^{1/2}}{m_t(E^2 + \Gamma_t^2)^{1/2} + m_H^2}, \quad (6)$$

to Eq. (5). This equation follows from writing the Yukawa potential in the form $\Delta\alpha_s(r)/r$. Fourier transforming, it is appropriate to evaluate this at the same momentum scale as in Eq. (5).

Figures 1 and 2 show representative plots of the cross sections. The mass of the Higgs particle and Λ were varied. The effects due to Higgs-boson exchange become almost negligible with $m_H > 100$ GeV. (Results received while this paper was being prepared for submission now suggest that $m_H > 41.6$ GeV.¹⁶) Λ was set equal to 0.1, 0.2, and 0.3 GeV.

The calculations of Fadin and Khoze neglect the effects of long-range confining forces. To estimate the importance of such forces, the production cross section was calculated using an effective α_s^R corresponding to the Richardson potential, which includes these effects. This model is an extreme case in that $\Lambda_R = 0.375$ GeV, a value

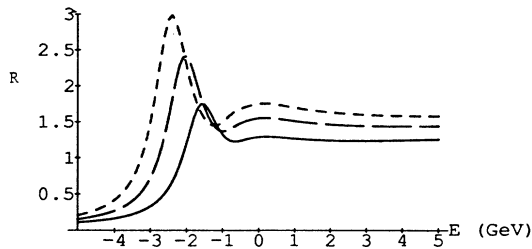


FIG. 1. Plots of the production cross section for various values of Λ with $m_t = 140$ GeV and $m_H = 50$ GeV ($\Lambda = 0.1$ GeV: solid; $\Lambda = 0.2$ GeV: long dashes; $\Lambda = 0.3$ GeV: short dashes). $E = \sqrt{s} - 2m_t$.

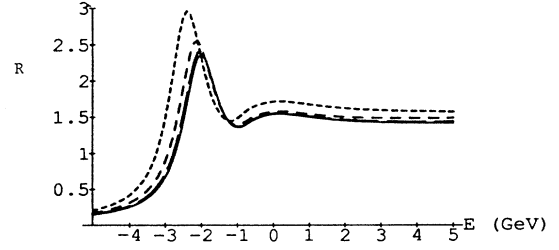


FIG. 2. Plots of the cross section for various values of m_H with $m_t = 140$ GeV and $\Lambda = 0.2$. ($m_H = 100$ GeV: solid; $m_H = 50$ GeV: long dashes; $m_H = 25$ GeV: medium dashes; $m_H = 0$ GeV: short dashes.)

much higher than the values of the parameter typically used. The coupling constant is then given by

$$\alpha_s^R = \frac{12\pi}{(22 - 2n_f) \ln[1 + m_t(E^2 + \Gamma_t^2)^{1/2}/\Lambda_R^2]} \quad (7)$$

with $n_f = 5$.¹² Figure 3 shows a comparison of the cross section using the Richardson potential and the cross section with one-gluon exchange and $\Lambda = 0.375$ GeV. There is no readily perceptible difference between the two plots, so the long-range effects do not have a major effect on $R_{t\bar{t}}$ in this range for m_t ; for examples of where they can be important see Ref. 13.

The figures show the obvious effects of both decreasing m_H and increasing Λ . Production of toponium is increased, and the energy values (measured horizontally) of the peaks decrease. As one might expect, since changes in both variables have largely the same result, plots with different combinations of Λ and m_H can be very similar. For example, Fig. 4 compares a plot with $\Lambda = 0.2$ GeV and $m_H = 0$ to one with $\Lambda = 0.3$ GeV and $m_H = 50$ GeV. Close examination of this figure will reveal minor differences especially in the secondary "bump" of both graphs. In the plot with $\Lambda = 0.3$, the production is slightly higher there. It is apparently true in general that the cross section is higher in the subsidiary maximum for greater Λ when the height of the first peak is the same. However, the deviation is probably not large enough for it to be

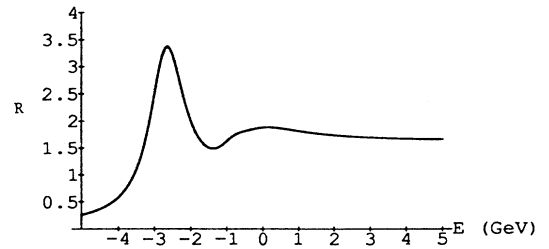


FIG. 3. Comparison of plots of the cross section using the Richardson potential and a potential with one-gluon exchange with $m_t = 140$ GeV, $m_H = 50$ GeV, and $\Lambda = 0.375$ GeV.

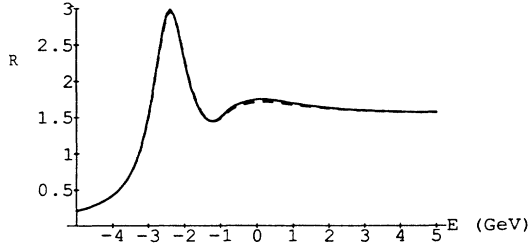


FIG. 4. Comparison of plots of R_{ii} for $m_t = 140$ GeV with $\Lambda = 0.2$ GeV and $m_H = 0$ (dashed) and with $\Lambda = 0.3$ GeV and $m_H = 50$ GeV (solid).

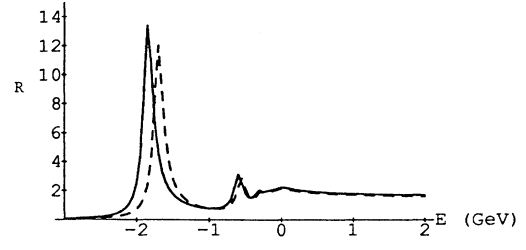


FIG. 5. Plots of the cross section for $m_t = 100$ GeV and $\Lambda = 0.2$ GeV with $m_H = 0$ GeV (solid) and $m_H = 100$ GeV (dashed).

exploited in order to determine how much of the shift in peaks is due to Λ and how much is due to the Higgs-boson exchange. Of course, by the time that the data has been collected, the Higgs-boson mass will have been determined if the effects are non-negligible.

For a given set of data, the domain of m_H seems to span a range for Λ on the order of 0.1 GeV wide. However, the shift in position from $m_H = 0$ to $m_H = \infty$ seems to decrease with smaller values of Λ .

III. EIGENVALUE CALCULATIONS

The energy eigenvalues were calculated for values of the principal quantum number up to three with no orbital angular momentum ($l = 0$). These may be used as a check on the cross-section calculations since the spacings between different eigenvalues should correspond to the distance between peaks in the plot of R_{ii} . This is important since decay widths and production cross sections depend crucially on the quarkonia wave functions.¹³

The eigenvalue calculations were carried out using the Wisconsin potential V_{Wis} , rather than the simple potential for the one-gluon exchange or V_R since its expres-

sion was easier to deal with in configuration space. V_{Wis} includes a term that is linear with respect to distance, so it includes long-range effects just as V_R does. With $\Lambda = 0.2$ GeV, V_{Wis} still fits the data well where as the most likely value of Λ_R is 0.375 GeV. Thus, V_{Wis} is probably a more realistic potential than either V_R or that based on single-gluon exchange. The contribution to the potentials due to Higgs-boson exchange were included by adding a Yukawa term:

$$V(r) = V_{Wis}(r) + \frac{\sqrt{2}G_F m_t^2 e^{-m_H r}}{4\pi r}. \quad (8)$$

The calculated eigenvalues for the $1s$ state and the spacings between the $1s$, $2s$, and $3s$ states are listed in Table I. We used a shooting method to solve the radial Schrödinger equation. In this table, $\Lambda = 0.2$ GeV. We used tridiagonal matrix methods¹⁷ to corroborate these results.

Only the cross section plots for a 100-GeV top quark provided enough peaks to make a comparison with the eigenvalue data. The deviation in the $1s$ peak between the two methods was small (See Fig. 5). The eigenvalue data undervalued the spacing between the $1s$ and

TABLE I. Eigenvalue spacings for $1s$, $2s$, and $3s$ states in GeV.

m_H (GeV)	State	$m_t = 100$ GeV	$m_t = 140$ GeV	$m_t = 180$ GeV
0	$1s$	-1.7370	-2.2764	-2.9625
	$2s-1s$	0.9550	1.2618	1.7007
	$3s-1s$	1.3584	1.7025	2.2059
50	$1s$	-1.6199	-1.9734	-2.3388
	$2s-1s$	0.8820	1.0643	1.2853
	$3s-1s$	1.2705	1.4671	1.7096
100	$1s$	-1.6141	-1.9505	-2.2745
	$2s-1s$	0.8777	1.0461	1.2323
	$3s-1s$	1.2656	1.4469	1.6515
∞	$1s$	-1.6114	-1.9386	-2.2387
	$2s-1s$	0.8758	1.0369	1.2037
	$3s-1s$	1.2634	1.4367	1.6197

2s states by about 20% and the spacing between the 1s and 3s states by 5–10%. This is very good agreement considering the major differences between the two methods used.

IV. CONCLUSION

Higgs-boson exchange can be a non-negligible factor in the process $e^+e^- \rightarrow t\bar{t}$ if the mass of the top quark is around 140 GeV and the Higgs boson is sufficiently light.

The most recent lower bounds on the Higgs-boson mass seem to place serious constraints on the magnitude of the effect that can be expected when toponium is produced.

ACKNOWLEDGMENTS

I am deeply indebted to C. Taylor for his advice and encouragement. The Physics Department of Case Western Reserve University provided the funding for this project.

*Present address: Department of Physics and Astronomy, State University of New York at Buffalo, Buffalo, NY 14260.

¹J. H. Kühn and P. M. Zerwas, Phys. Rep. **167**, 321 (1988).

²CDF Collaboration, H. B. Jensen, Bull. Am. Phys. Soc. **35**, 943 (1990).

³W. Marciano, Electroweak Working Group Summary, Snowmass Conference, 1990 (unpublished).

⁴K.-I. Hikasa, in *Towards TeV Physics*, proceedings of the Workshop, Tsukuba, Japan, 1990 (KEK Report No. 90-18, Tsukuba, 1990).

⁵I. Bigi *et al.*, Phys. Lett. B **181**, 157 (1984).

⁶M. Sher and D. Silverman, Phys. Rev. D **31**, 95 (1985).

⁷G. Athanasiu, P. Franzini, and F. Gilman, Phys. Rev. D **32**, 3010 (1985).

⁸H. Inazawa and T. Morii, Phys. Lett. B **203**, 279 (1988).

⁹H. Inazawa and T. Morii, Z. Phys. C **42**, 563 (1989).

¹⁰V. S. Fadin and V. A. Khoze, Pis'ma Zh. Eksp. Teor. Fiz. **46**, 417 (1987) [JETP Lett. **46**, 525 (1987)]; Yad. Fiz. **48**, 487 (1988) [Sov. J. Nucl. Phys. **48**, 309 (1988)].

¹¹K. Hagiwara *et al.*, Phys. Lett. **130B**, 209 (1983).

¹²J. L. Richardson, Phys. Lett. **82B**, 272 (1979).

¹³V. Barger *et al.*, Phys. Rev. D **35**, 3366 (1987).

¹⁴A. D. Martin and A. W. Peacock, Z. Phys. C **33**, 135 (1986).

¹⁵K. Fujikawa, Prog. Theor. Phys. **61**, 1186 (1989).

¹⁶ALEPH Collaboration, D. Decamp *et al.*, Phys. Lett. B **246**, 306 (1990).

¹⁷K. J. Miller and M. G. Olsson, Phys. Rev. D **25**, 2383 (1982).